General Disclaimer

One or more of the Following Statements may affect this Document

- This document has been reproduced from the best copy furnished by the organizational source. It is being released in the interest of making available as much information as possible.

- This document may contain data, which exceeds the sheet parameters. It was furnished in this condition by the organizational source and is the best copy available.

- This document may contain tone-on-tone or color graphs, charts and/or pictures, which have been reproduced in black and white.

- This document is paginated as submitted by the original source.

- Portions of this document are not fully legible due to the historical nature of some of the material. However, it is the best reproduction available from the original submission.

Rensselaer Polytechnic Institute

Troy, New York

R.P.I. Technical Report MP-7

THE DESIGN STUDY OF A LIGHTWEIGHT ROTOR HUB FOR A MARS-LANDING AUTOGYRO

by

Wilson Parker Rayfield

NASA Grant NGL 33-018-091

Analysis and Design of a Capsule Landing System
and Surface Vehicle Control System for Mars Exploration

SEPTEMBER 1969

Rensselaer Polytechnic Institute
Troy, New York

CONTENTS

LIST OF TABLES

LIST OF FIGURES

I. INTRODUCTION

One major objective of the United States space program during the next few decades will be the exploration of the planet Mars. Under contract with the National Aeronautics and Space Administration, several Mars-oriented projects are being directed by Dr. Stephen Yerazunis at Rensselaer Polytechnic Institute. Dr. George N. Sandor, chairman of the Machines and Structures Division, is supervising one task group with the project goal of designing the means for final descent and soft-landing of a 150-pound instrument package on Mars.

The Martian atmosphere is quite tenuous, about one-hundredth the surface density of the earth; this precludes the use of parachutes for a soft-landing. Retrorockets may alter the immediate area to be investigated, and due to the weight limitations could not provide alone the deceleration necessary during the entire descent. A further difficulty is the existence of strong, gusty surface winds, averaging 200 feet per second.[4]*

To overcome these problems an unpowered autogyro has been proposed.[4] Making use of lightweight, inflatable plastic rotor blades, the landing capsule could be stowed, blades deflated, in a Martian orbiter package for the voyage from earth to Martian orbit. When deployed from the orbiter, the capsule would assume a decaying, entry trajectory. Upon inflation of the rotor blades, the landing capsule would act like a shuttlecock at the first traces of

*Superscripted numbers refer to section IX. Literature Cited

atmosphere; the blades would cone back and create a drag force for initial deceleration. By adjusting the blade pitch, rotation could be induced; this would create a centrifugal force component on the blades, spreading them over a larger generated circle. Gradually the rotor would increase in speed, further spreading the blades, until autorotation is reached.

As the capsule neared the surface, the cyclic blade pitch could be adjusted to counteract the surface winds. Firing a tethered anchor to the surface would provide a stabilizing guide to land. At this point a small pitch adjustment could convert the stored kinetic energy of the spinning rotor into a final deceleration thrust for a gentle touch-down.

For this concept to be useful, it must be possible to design a practical rotor and rotor hub at a reasonable payload fraction.

The rotor-hub assembly would have to provide control of both the cyclic and collective blade pitches, monitoring of the coning angle of the blades, and include a highly reliable, low friction rotor bearing.

The design would have to withstand the temperature range and vacuum of space, be sterilizable, and be extremely lightweight.

II. ROTOR BEARING

Design Limitations

The rotor bearing is the most critical component of the rotor-hub assembly, and must function flawlessly during the descent. The axial loading on the bearing will vary from zero initially, to 50 pounds, the Martian weight of the capsule and hub to be supported, when autorotation speed is reached; the final deceleration just before landing may produce a 12 g_m axial load of 600 pounds. The bearing must also withstand any lateral loading which may occur.

The rotor speed will also vary during the landing. Increasing from zero to an average of 100 rpm, and a maximum of 250 rpm, the rotor bearing must transmit as little moment as possible to the descending craft.

Other design considerations include the size and weight limitations imposed on the entire design, and lubrication restrictions of a vacuum environment.

Hydrostatic Bearing

A gas-lubricated hydrostatic bearing possesses many of the features required for the main hub bearing. A lubricating gas is supplied under pressure through a resistance to the narrow space between the bearing surfaces and escapes into the surrounding atmosphere. Figure 1 shows the pressure distribution across a conical hydrostatic bearing with a ring of supply jets. Hydrostatic bearings

FIGURE 1: PRESSURE DISTRIBUTION
CONICAL HYDROSTATIC BEARING

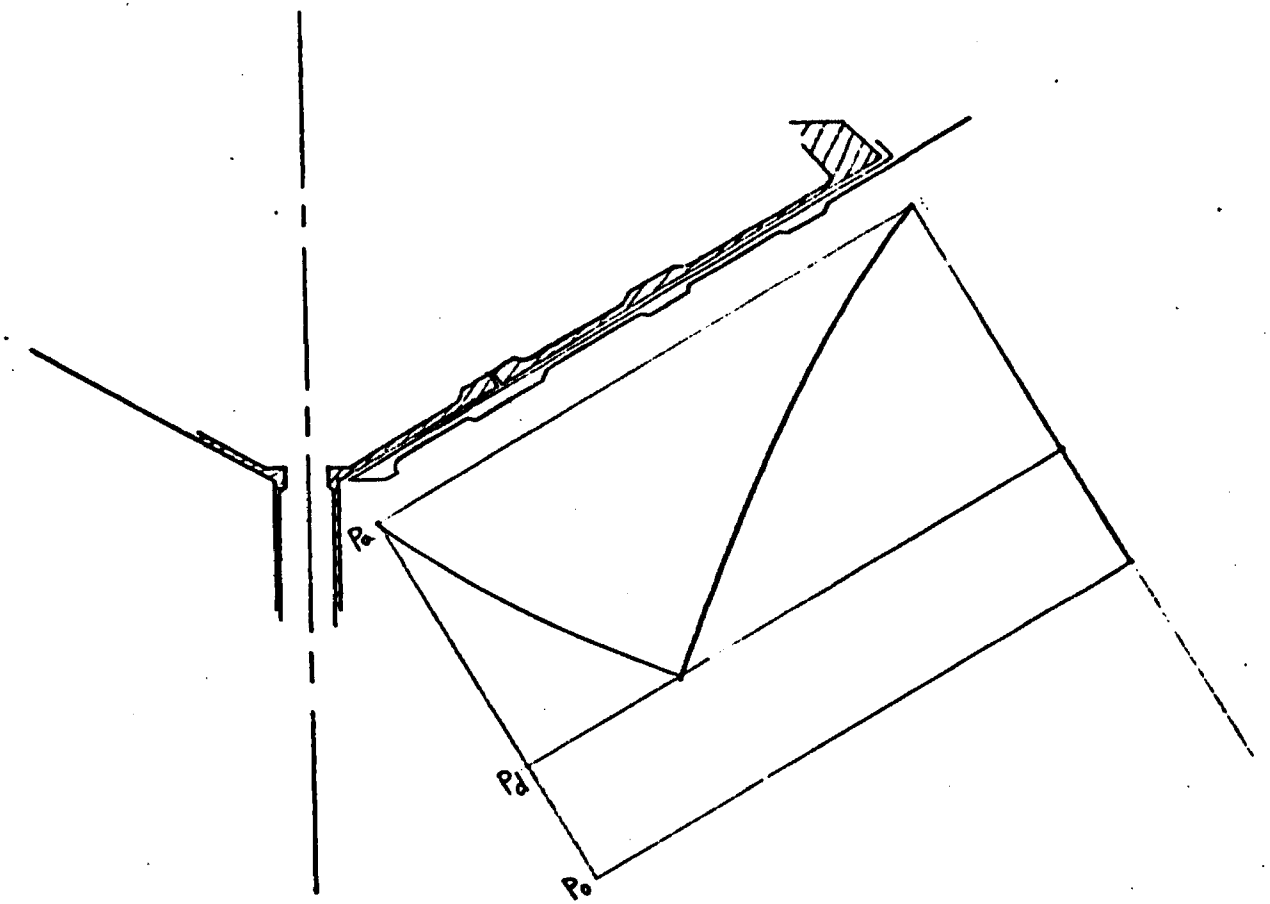

will function with a mimimum of friction at standstill to moderate speeds, and adjust automatically to carry increasing or decreasing loads. As the load increases, for example, the gap width between surfaces is decreased, adding resistance to the gas flow; this causes a smaller pressure drop across the supply resistor, increasing the pressure at which the gas enters the gap, and thus allows the bearing to support the heavier load. When the load decreases, the gap widens, the gas flow resistance decreases, the pressure drop across the supply resistor increases, and the bearing pressure force thus adjusts to equal the decreased load. Figure 2 shows how the bearing gap varies with the applied load.[9]

The bearing is stiffest at the point on the graph where the slope is steepest; it is desirable to design the bearing such that the maximum load occurs at this stiffest point.

A cone shaped bearing was chosen for three reasons. It provides for both the major axial loading and the smaller lateral loading, is self-alligning, and can be machined to the close tolerances necessary.

The cone size was optimized to accomodate the large blade hinges and maximum thrust, and also to minimize the bearing weight.

Since the allowable thrust is a function of the cones' vertically projected area, the conical height and angle may be adjusted to reduce the weight of the cones.

The lubricating gas is fed to the bearing through

FIGURE 2 : VARIATION OF PRESSURE FACTOR WITH CLEARANCE

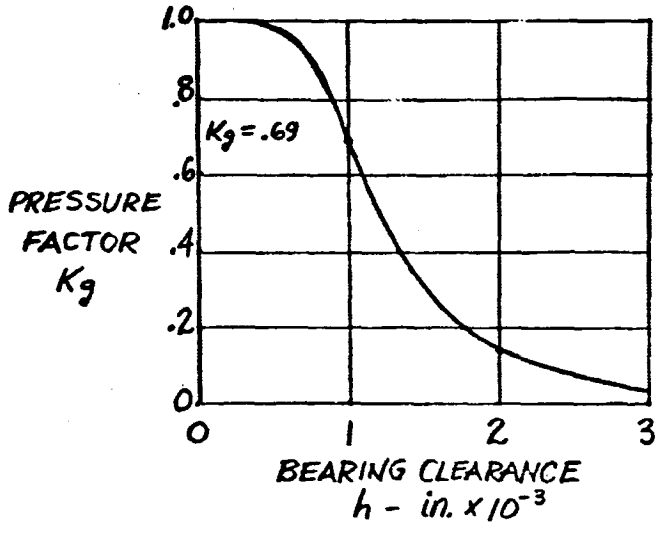

TABLE 1 : SUPPLY PRESSURE NECESSARY FOR VARIED CONE SIZES

K_g	W_M (POUNDS)	a (INCHES)	b (INCHES)	P_o (PSI)
PRESSURE FACTOR	MAXIMUM AXIAL LOAD	CONE RADIUS AT APEX OUTLET	CONE RADIUS AT BASE OUTLET	SUPPLY PRESSURE NECESSARY
.69	600	1.0	3.0	47.7
.69	600	1.0	5.0	27.9
.69	600	1.0	9.0	9.5
.69	600	1.0	12.0	5.7

small tubes from a gas supply inside the capsule. The tubes are anchored to the inside wall of the inner bearing cone and pass through a small cylindrical neck joining the inner cone to the capsule.

For the following calculations, these assumptions were made:

The lubricating gas was assumed to be incompressible, since this introduces only small errors and greatly simplifies the calculations.[9]

The temperature in the lower atmosphere and on the surface of Mars was assumed constant at 0°C.[4]

The viscosity of the lubricating gas was assumed constant.

The gravitational acceleration of Mars was assumed constant at g_m = 12.3 ft. / sec.^{2} [4]

The discharge jets are placed such that the gas flow is equal in both the apex and base directions.

The maximum deceleration was assumed to be 12 x g_m.

The atmospheric pressure on Mars, estimated to be .145 psi at the surface[4] was assumed to be constant; this assumption introduces negligible error, since the equations depend upon the difference between this pressure and the supply pressure, which is two orders of magnitude larger.

Known parameters:

W_{av} = 50 lbf., average axial loading, Martian weight of capsule and hub to be supported.[4]

W_m = 600 lbf., maximum axial loading at 12 x g_m.

P_a = .145 psi, Martian atmospheric pressure

T = 0°C, average Martian surface temperature

Unknown parameters:

θ, conical angle

a, cone radius at apex outlet

b, cone radius at base outlet

$c = \sqrt{ab}$, radius of circle of supply jets

n, number of supply jets

d, diameter of supply jets

p_o = supply pressure

Unknown variables:

h, axial film thickness

p_d, jet discharge pressure

C_d, supply jets' discharge coefficient

m, mass flow rate

Integrating the pressure over the conical surface area yields the following equation:[9]

$W_m = K_g (p_o - p_a) \frac{\pi (b-a)^2}{\ln (b/a)}$, where K_g is the pressure factor, $K_g = \frac{p_d - p_a}{p_o - p_a}$; $K_g = .69$ at the point of maximum stiffness, or steepest slope in figure 2. Letting this point indicate the maximum load, corresponding values of the unknowns may be determined, as shown in table 1. Providing a large enough cone for mounting the blade hinges in an integral structure, maintaining a relatively low pressure requirement, and seeking a reduced weight led to the choice of the 9-inch cone for further analysis.

The mass flow rate for a conical thrust bearing with a ring of jets is given by:[9]

$M = \frac{\pi h^3 g_c (p_d^2 - p_a^2) \sin \theta}{3 \mu R T \ln (b/a)}$. Assuming a conical angle of 60°; a film thickness of .001 inch and discharge pressure of 6.55 psi ($p_d = .69\ p_o$), both corresponding to the maximum load configuration; and the lubricating gas to be air, with a viscosity at 0° C equal to 1.165×10^{-5} lbm./ft.sec., and gas constant equal to 53.36 lbf.ft./lbm.°R; the mass flow rate can be calculated:

$$m = \frac{\pi(5.78\times10^{-13}\ \text{ft.}^3)(32.2\ \text{ft.lbm./sec}^2\text{lbf.})(8.9\times10^5\ \text{lbf.}^2/\text{ft.}^4)(.866)}{3(1.165\times10^{-5}\ \text{lbm./ft.sec.})(53.36\ \text{lbf.ft./lbm.°R})(492\text{°R})(2.2)}$$

$= 2.26 \times 10^{-5}$ lbm./sec.

Assuming a descent operational time of 500 seconds, the bearing would require only 1.13×10^{-2} lbm. of air. At the low supply pressure, 9.5 psi., and the temperature range expected, the weight and space allotment of the gas storage system should pose no problem. The additional gas supply necessary for a possible relift and relocation maneuver would likewise be comparatively small.

The bearing slot factor, G, related to K_g by:[9]

$K_g = \dfrac{2}{1 + (1 + 4/G^2)^{\frac{1}{2}}}$, will be 1.25 when K_g is 6.9. The bearing slot factor, expressed in terms of the bearing parameters, yields:[9]

$$G = \frac{p_a/p_o}{(1-p_a/p_o)^{\frac{1}{2}}(1+p_a/p_o)} \cdot \frac{24\mu\,(2\,g_c\,R\,T)^{\frac{1}{2}}}{p_a\,g_c} \cdot \frac{C_d\,n\,d^2\,\ln(b/a)}{32\,h^3}.$$

With six equally spaced jets, n = 6, assuming a discharge coefficient of unity, $C_d = 1$, the optimum jet diameter is found to be 4.34×10^{-3} inch.

Integrating the shear stress on the bearing area, assuming a constant shear rate across the bearing gap, permits the transmitted moment to be calculated:[10]

$M = \dfrac{\pi\mu W (b^4 - a^4)}{2\,g_c\,h\,\sin^2\theta}$. This moment is a maximum when the thrust load on the bearing is a maximum, at which point the bearing speed is 250 rpm, and h = .001 inch. Thus, for the 12 g_m load, the maximum transmitted moment is .902 in.lbf.

To counter this torque a small deployable stabilizer fin is attached to the capsule body. This fin is

adjustable about the horizontal shaft by which it is mounted; as the capsule descent speed decreases or the thrust increases, the fin rotates to a greater angle from the vertical to balance the net torque on the capsule. See figure 3.

Vibration-induced Squeeze-film Bearing

The application of vibration-induced squeeze-film bearing theory to the design of the main rotor bearing has been investigated. The electrically induced high-frequency oscillation of a piezoelectric ceramic attached to a bearing surface acts as a pump on the ambiant atmosphere to hydrostatically lubricate the bearing. The main advantage of such a system is that it requires no stored gas supply, as with the standard hydrostatic bearing. The squeeze-film bearing is also compact, simple, and easy to regulate. An experimental conical squeeze-film bearing diagram and a schematic of the wave extender, used to amplify the ceramic's vibration, are shown in figures 4 and 5.[13]

The main limitation of the squeeze-film bearing is that the ambiant pressure must be approximately three times the needed bearing pressure.[13] The support of the capsule load at 1 g_m, 50 pounds Martian weight, with the present rotor configuration would require an ambiant pressure on Mars of .569 psi. However, this value is estimated at approximately .145 psi, which would require a cone of nearly twice the size of the present design. Not only would this greatly increase the hub weight, a critical design factor, but such a bearing would be useless at the high descent altitudes

FIGURE 3: MOMENT-STABILIZER FIN LAYOUT

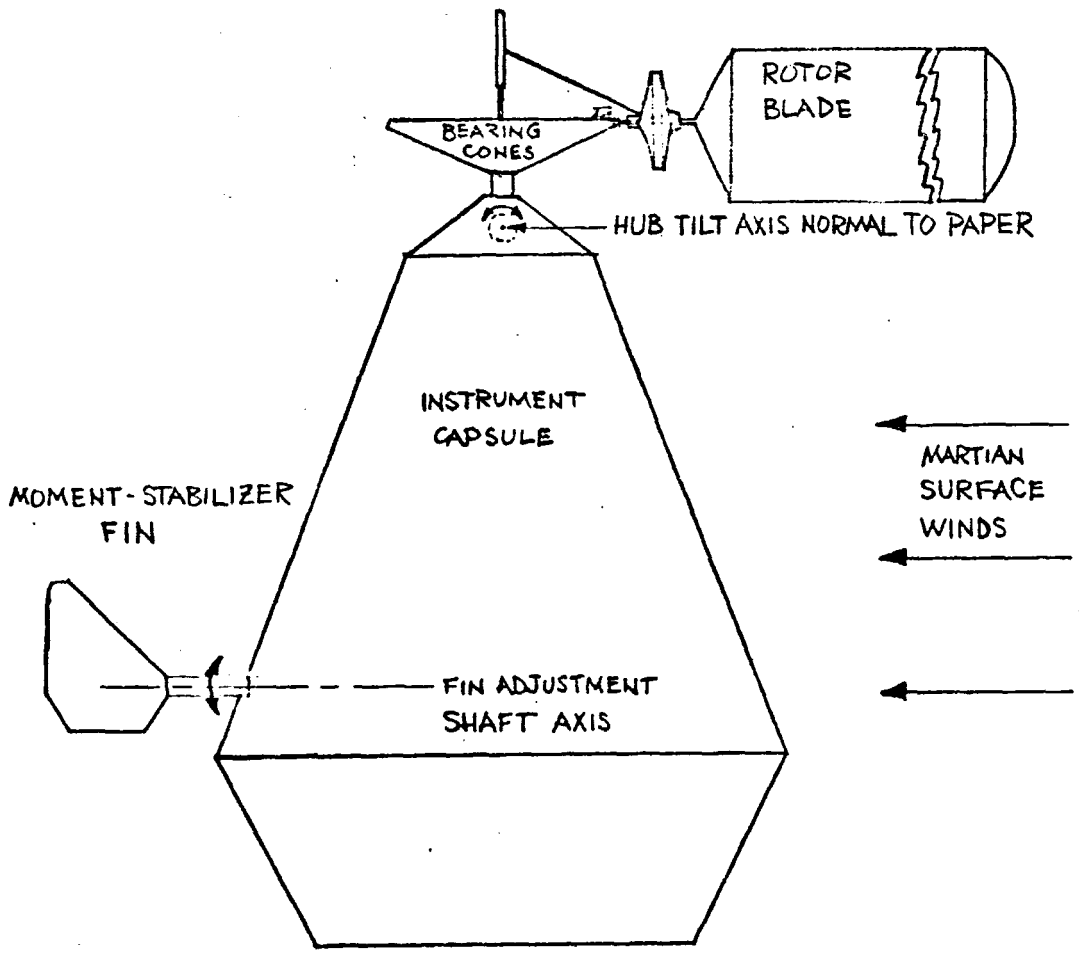

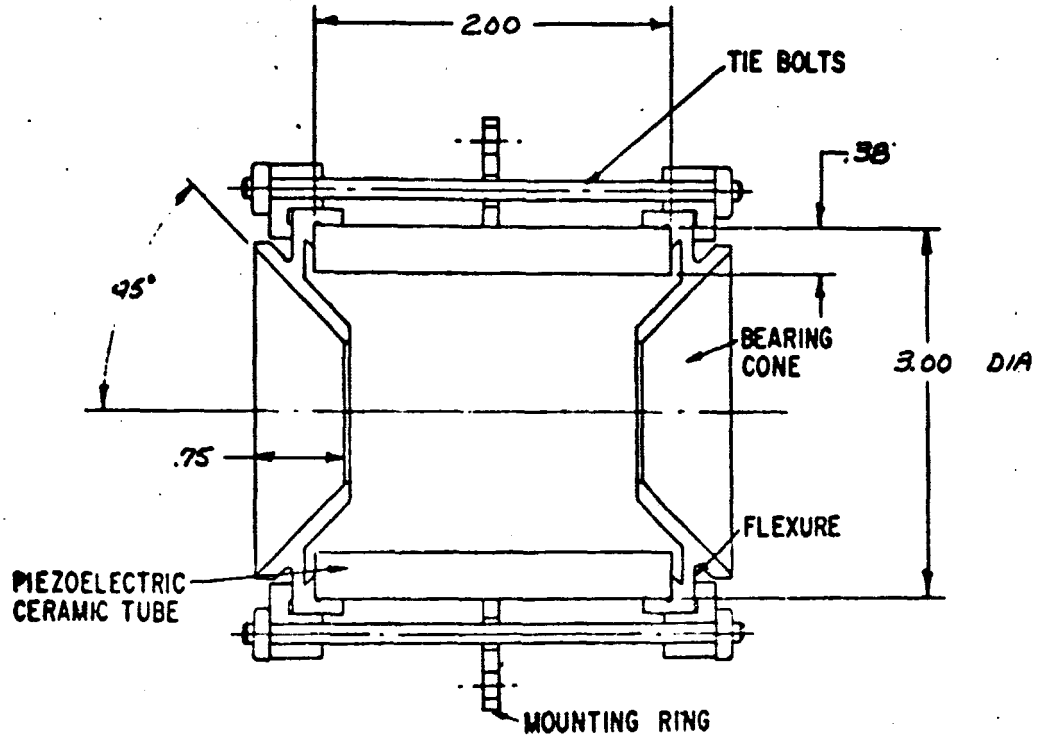

FIGURE 4. EXPERIMENTAL AXIAL-EXCURSION CONICAL SQUEEZE-FILM BEARING WITH WAVE-EXTENDER TYPE TRANSDUCER

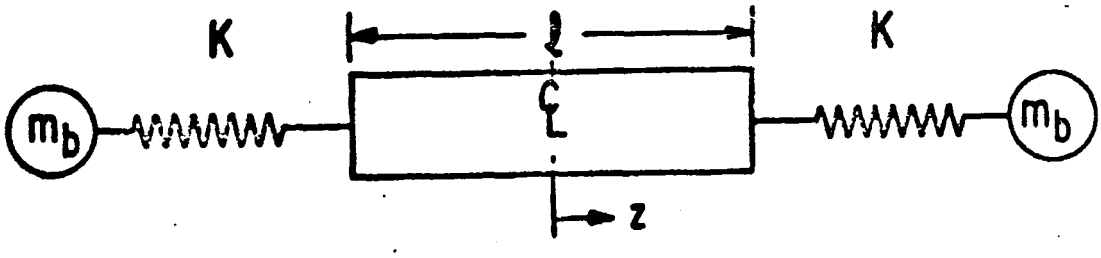

FIGURE 5. SCHEMATIC OF WAVE EXTENDER

where the ambiant pressure is much less than on the Martian surface, and would not carry the deceleration thrust loads at lower altitudes.

Applying the theory to our present nine-inch radius cones, and with the surface pressure of .145 psi, the squeeze-film bearing could support about 13 pounds of the 50-pound average load, as shown in figure 6. By superposition with the present hydrostatic bearing design, the combined bearing would help conserve the lubricating gas supply during operation on or close to the surface of Mars. Reducing the load carried by the hydrostatic portion would reduce the required gas supply pressure. The volume flow rate would thus decrease, and, since the lower pressure would reduce the gas density, the mass flow rate would decrease even more. Thus the combined bearing, it was found, would extend the life of the original hydrostatic bearing by about one-half. See table 2.

The addition of the squeeze-film bearing would add a small amount of weight for electronic equipment, and require some modifications in the rotor hub design. Figure 7 shows two possible design orientations incorporating the piezoelectric ceramic into the cone shaft. It was found that the ceramic was adequately strong to be used in tension, which has one-tenth the design stress limit of the compressive orientation.

FIGURE 6: SQUEEZE-FILM BEARING PARAMETERS

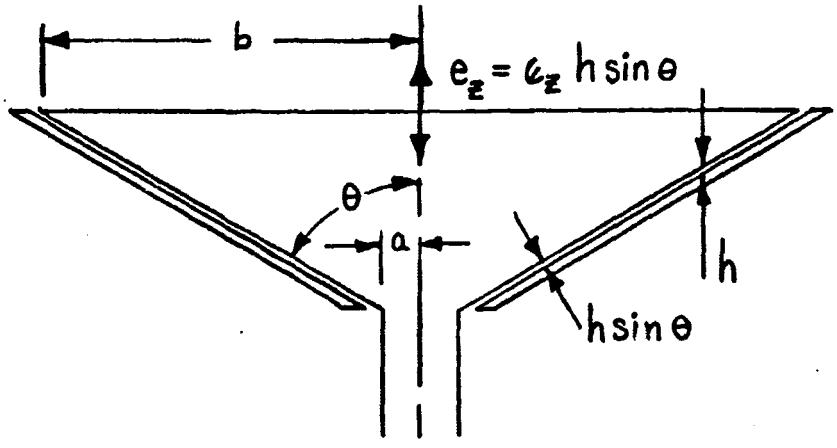

AXIAL LOAD = W = 50 LBF.
AXIAL EXCURSION = e_z
AXIAL EXCURSION RATIO = ϵ_z

LETTING $e_z = .5(h)$, $\epsilon_z \sin\theta = .5$

$$p_a = \frac{W}{A_z} \frac{1}{\sqrt{\frac{1 + 3/2\ \epsilon_z^2 \sin^2\theta}{1 - \epsilon_z^2 \sin^2\theta}} - 1}$$

WHERE p_a = AMBIANT PRESSURE
AND A_z = PROJECTED AREA OF CONE ON HORIZONTAL PLANE.
FOR $\theta = 60°$, $a = 1"$, AND $b = 9"$,
$p_a = .569$ psi, REQUIRED AMBIANT PRESSURE.

BUT MARTIAN AMBIANT PRESSURE (MAX.) = .145 psi;
NECESSARY A_z TO SUPPORT 50 LBF. LOAD IS 986 SQ.IN.
THIS AREA REQUIRES $b = 17.7"$, WITH $a = 1"$

FOR $a = 1"$, $b = 9"$, AND $p_a = .145$ psi,
THE BEARING CAN SUPPORT 12.74 LBF.

TABLE 2: COMPARATIVE BEARING LIFE

	AVERAGE LOAD CARRIED BY HYDROSTATIC BEARING (lbf.)	AVERAGE LOAD CARRIED BY SQEEZE-FILM BEARING (lbf.)	HYDROSTATIC DISCHARGE PRESSURE NECESSARY (psi)	MASS FLOW RATE ($\times 10^{-5}$ lbm./sec.)	BEARING LIFE (hr./lbm.)
HYDROSTATIC BEARING ACTING ALONE	50	0	.691	.671	41.4
COMBINED HYDROSTATIC AND SQUEEZE-FILM BEARING	37	13	.549	.423	65.7

FIGURE 7.

SQUEEZE-FILM ROTOR BEARING

STRUCTURAL LOAD ON TRANSDUCER
(PIEZOELECTRIC CERAMIC)

DESIGN TENSILE STRESS = $\sigma_T = 3.62 \times 10^3$ PSI
" COMPRESSIVE " = $\sigma_c = 3.62 \times 10^4$ PSI

CROSS-SECTIONAL AREA OF CERAMIC CYLINDER = A
WALL THICKNESS " " " = t
DIAMETER " " " = D = 2"

$$A = \frac{W_m}{\sigma} = \pi D t$$

$$t = \frac{W_m}{\sigma \pi D}$$

TENSION :

COMPRESSION:

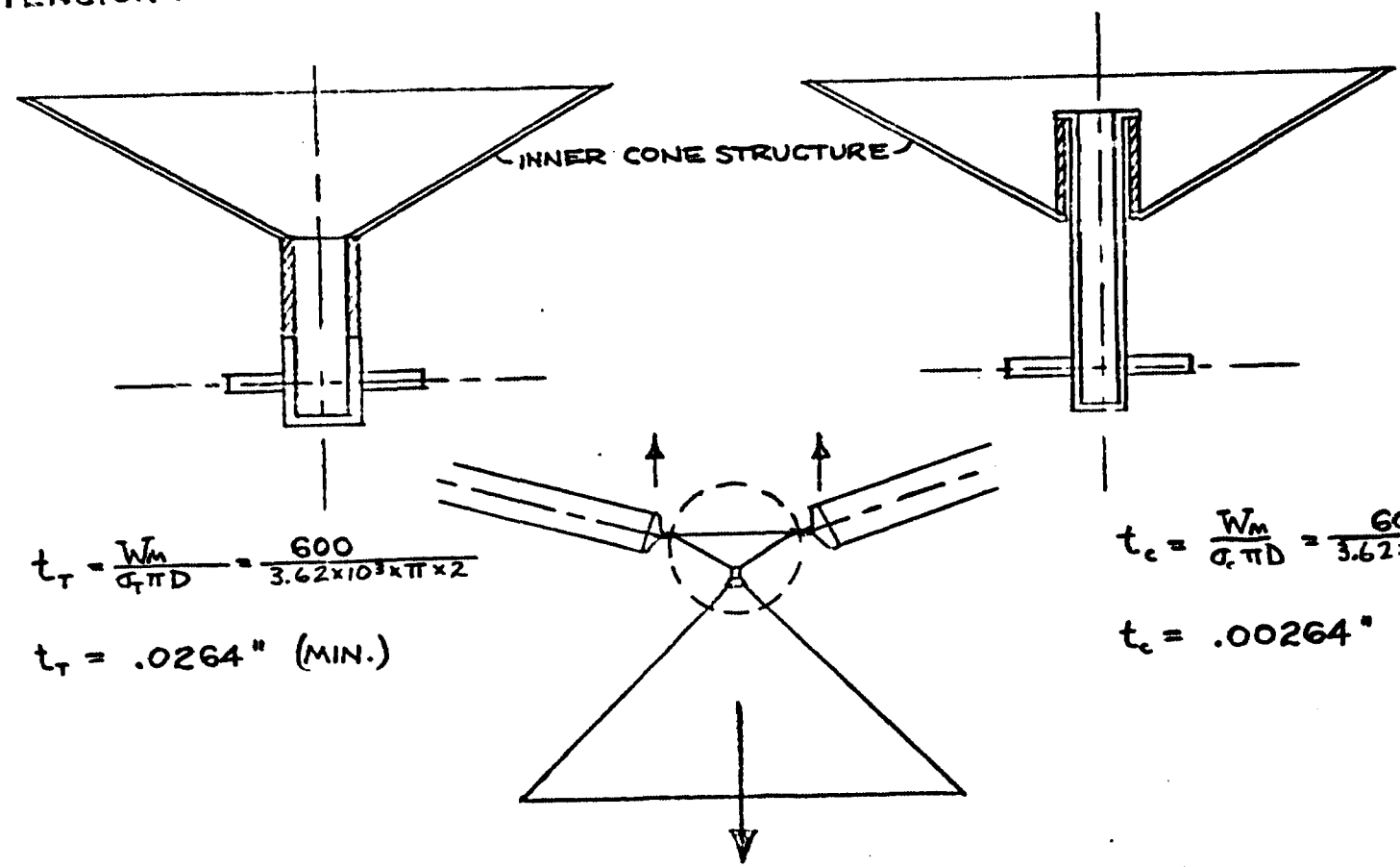

$$t_T = \frac{W_m}{\sigma_T \pi D} = \frac{600}{3.62 \times 10^3 \times \pi \times 2}$$

t_T = .0264" (MIN.)

$$t_c = \frac{W_m}{\sigma_c \pi D} = \frac{600}{3.62 \times 10^4 \times \pi \times 2}$$

t_c = .00264" (MIN.)

III. REVERSAL AND BACK-UP BEARINGS

Reversal Bearings

The normal loading on the conical thrust bearing will be such that the rotating outer cone will exert an upward force on the stationary inner cone. However, it is possible that this load may momentarily reverse during the descent, and of course will do so upon landing. To support this bearing load a reversal bearing system has been provided. Three solid-lubricant encased ball bearings are mounted on the upper rim of the inner hydrostatic-bearing cone. A teflon or nylon raceway[3] is mounted similarly on the rim of the outer cone structure. The reversal bearings and raceway are designed on the surface of a cone, inverted from the main bearing cones, so that they will provide both axial and lateral support. See figure 8.

Back-up Bearings

Since the rotor bearing is so critical to the mission, a back-up system has been incorporated in the hub design. Should the lubricating gas pressure supporting the hydrostatic bearing fall below the required level, a gas inflated diaphram would trigger a cocked spring or rolamite force generator[6] to actuate the back-up system. Each bearing is hinged such that when deployed and locked the bearings will have separated the inoperative prime bearing cones, preventing the smooth surfaces from binding. See figure 8.

The raceway for the back-up system is also

FIGURE 8 : REVERSAL AND BACK-UP BEARINGS

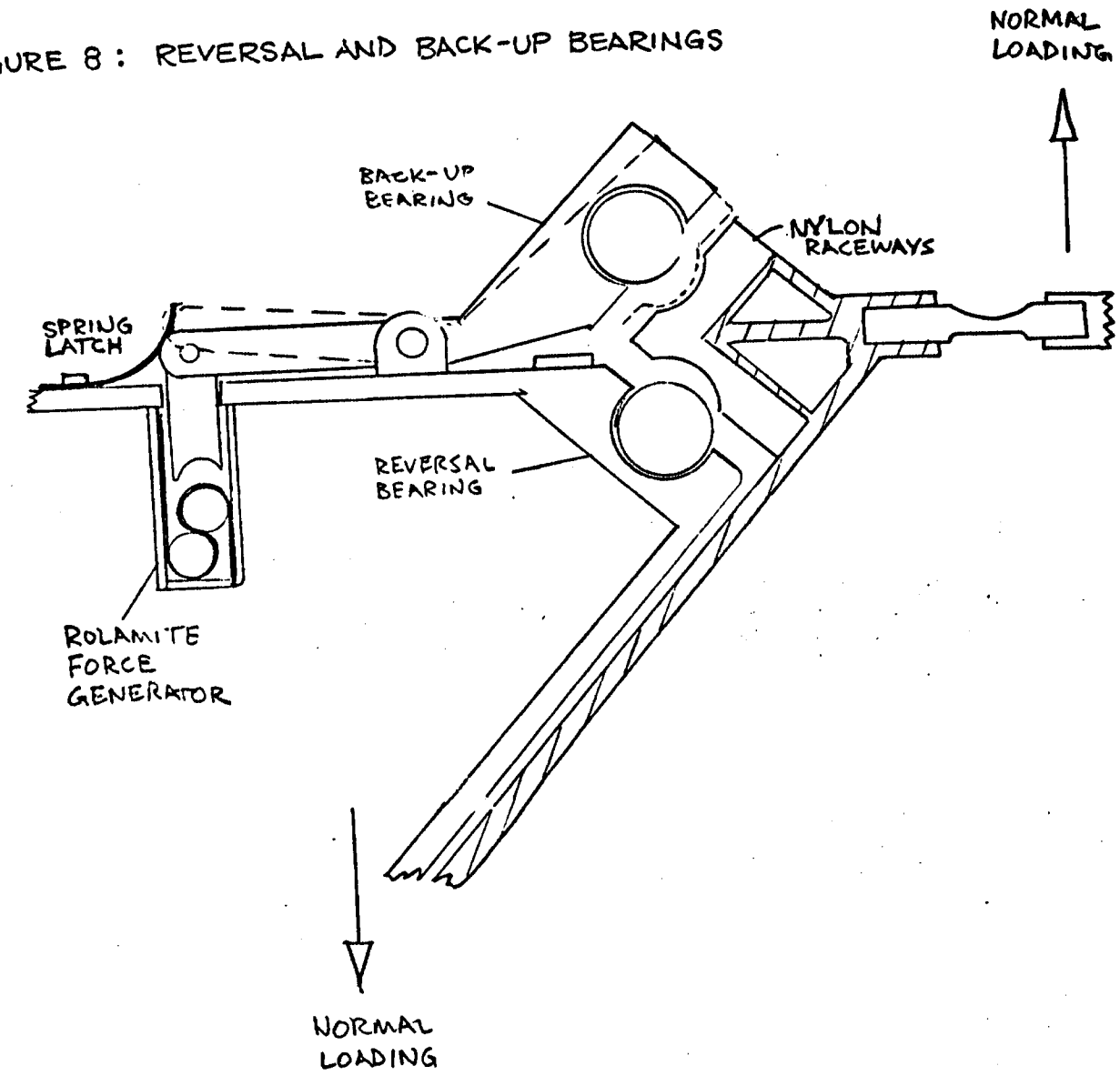

conical, inverted from that of the reversal bearings. However, to simplify construction and reduce weight, the two are made from an integral ring of plastic. Thus, both raceways can be mounted on the reinforced rim section of the outer cone structure.

IV. CYCLIC BLADE PITCH CONTROL

One element of the rotor hub operation which must be controlled during the descent is the cyclic blade pitch. This allows the autogyro to glide laterally while descending vertically. It is this property of the autogyro which allows it to counter the high velocity Martian surface winds.

The cyclic pitch control mechanism in classical rotor hub design involves a swashplate and cam mechanism. Because of friction and weight problems, magnified by space application, this approach was impractical. An alternative method, incorporated on small earth-use autogyros, is to tilt the entire hub about an axis perpendicular to the rotor axis; this automatically provides the cyclic pitch changes required.

By attaching the tilt-axis shaft to the cylindrical neck of the inner hydrostatic-bearing cone structure, the cyclic pitch bearings, actuating motor and control system can all be located within the pressurized capsule body; this greatly simplifies the design of the system. See figures 9a and 9b.

Since the orientation of the capsule with respect to the Martian winds can be maintained by the weathervane effect of the moment-stabilizing fin (figure 3), only one degree-of-freedom is required for the tilt mechanism: rotation about an axis perpendicular to the vertical plane containing the fin axis. A small electric D.C. motor driving a screw rod pivots the entire hub about the cyclic pitch tilt axis.

Figure 9a: Rotor-Hub Assembly

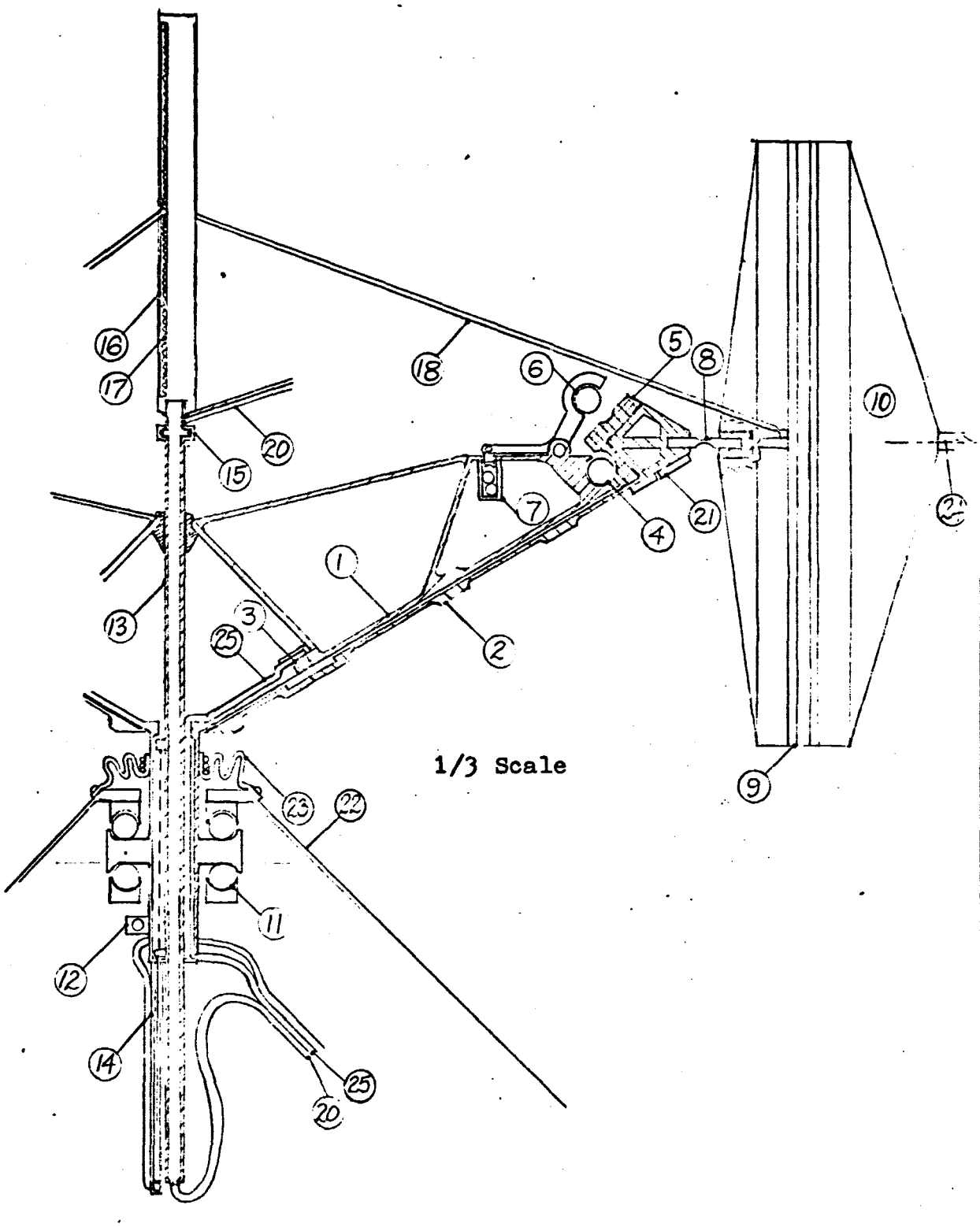

Figure 9b. ROTOR-HUB ASSEMBLY - KEY

1. Inner cone structure
2. Outer cone structure
3. Gas resistor discharge
4. Reversal bearing
5. Nylon roller surface
6. Back-up bearing
7. Rolamite force generator
8. Polypropylene flapping hinge (axial view)
9. Polystyrene lead-lag hinge (side view)
10. Mounting area for blade pitch bearings
11. Hub-tilt bearing
12. Hub tilt-actuator mount (threaded)
13. Coning angle indicator rod
14. Indicator tube
15. Swivel seal
16. Ball slot slides - indicator head
17. Averaging spring
18. Indicator spar
19. Indicator rod guide
20. Collective pitch control - reference pressure tubing (out of plane of indicator spar)
21. Fluidic pitch control element
22. Capsule body
23. Capsule flexible pressure seal
24. Blade pitch axis
25. Hydrostatic bearing gas supply tube

V. BLADE HINGES

Design Limitations

The autogyro rotor blades require three degrees of freedom: 90° vertical flapping in a plane through the rotor axis (coning angle), oscillation through a small angle about a vertical axis (lead-lag angle), and 360° rotation about their own longitudinal axis (pitch angle). The hinges necessary to provide these freedoms must withstand the lubrication restrictions of space, be lightweight, and endure the fatigue loading of the oscillating blades. Figure 10 shows the hinge orientation desired.

Pin type hinges are impractical due to their large friction areas; knife-edge pivots would wear quickly under the concentrated load; and solid lubricant bearings could not withstand the blade loading and meet the weight limitations.

Thermoplastic Hinges

Newly developed thermoplastic integral hinges were selected to meet the requirements and restrictions of this application. Formed from a single piece of plastic, these hinges have no friction surfaces to require lubrication, have a long fatigue life, and are lightweight. Figure 11 shows the cross-section of an integral hinge.[15]

Polypropylene is the most common plastic used, although polystyrene hinges have been developed incorporating a desired spring constant in the hinge. This would lend

FIGURE 10: BLADE HINGE CONFIGURATION

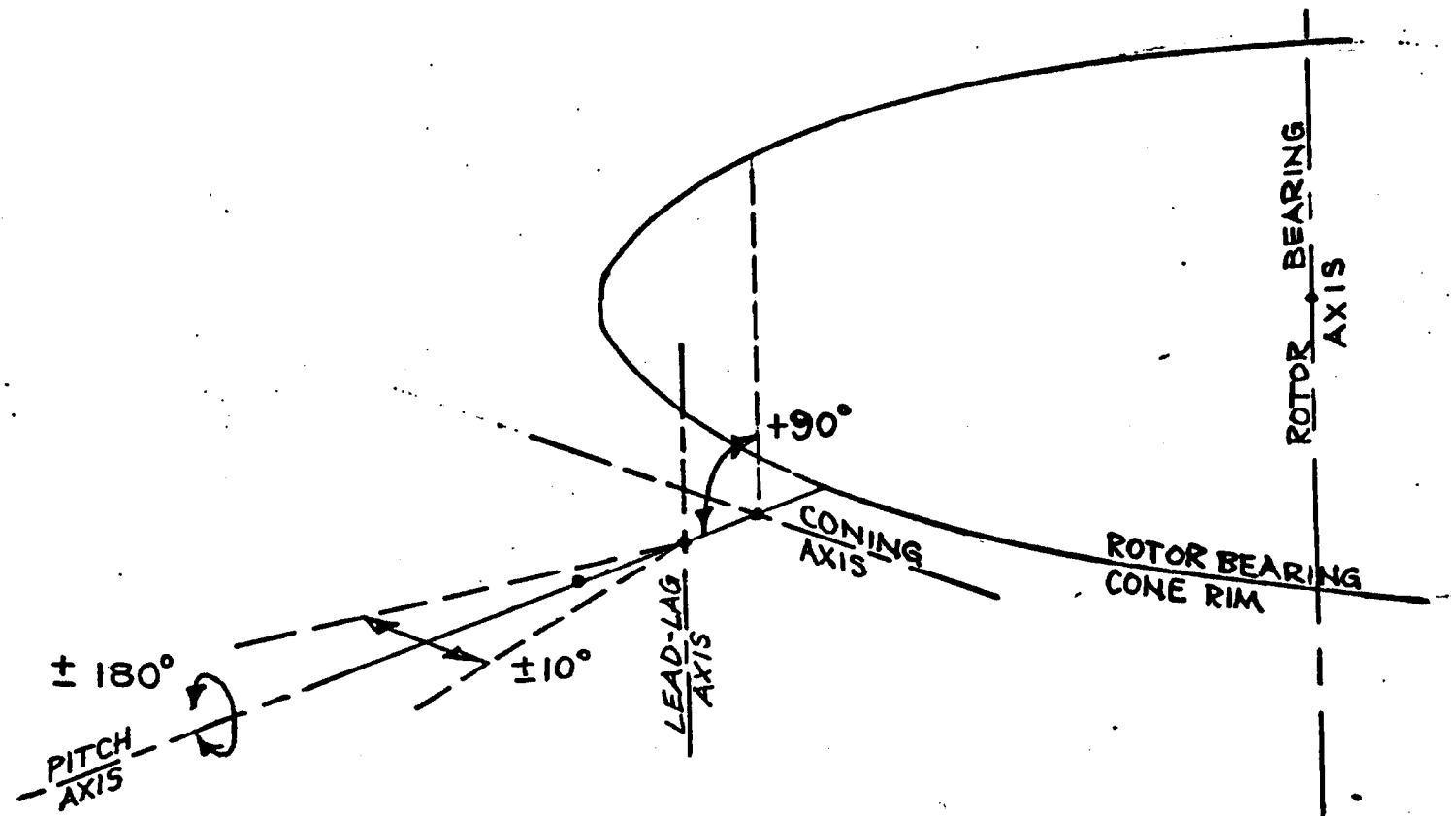

FIGURE 11 : POLYPROPYLENE INTEGRAL HINGE
(AXIAL VIEW)

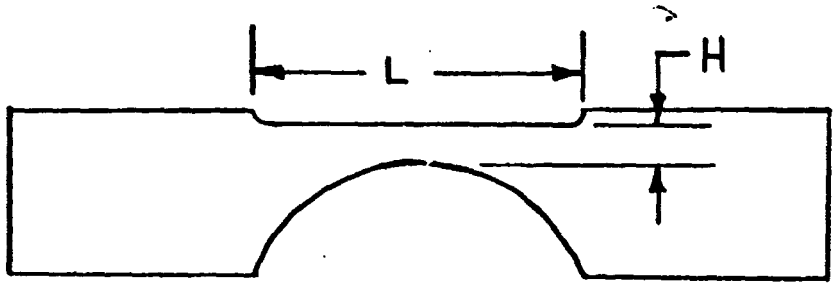

DESIGN LIMIT :

$L > 4H$

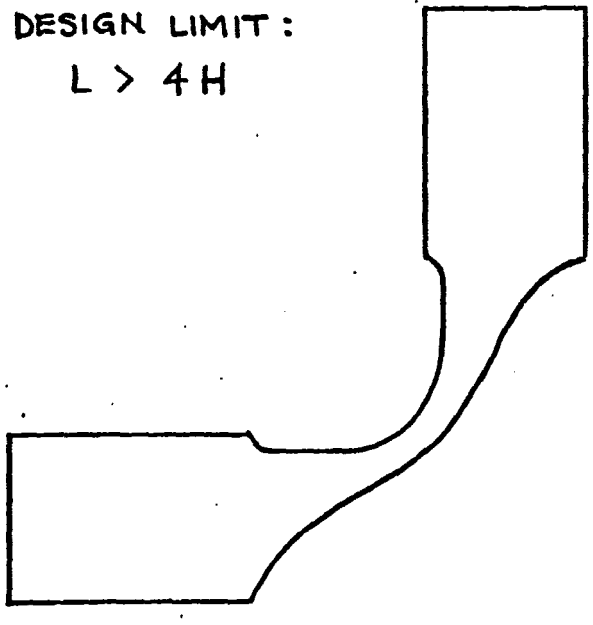

itself for use as a lead-lag hinge, since the autogyro design requires a spring restraint on this small-oscillation hinge. The flapping hinge must allow the blades to cone back freely during the initial descent stage, allowing the use of the polypropylene hinge.

The centrifugal force of the lightweight inflated blades was calculated to be greater than the thrust loads. Integrating over a 20 foot length blade, the centrifugal forces generated for each of the three proposed blade designs[14] are listed in table 3. The variation of the coning angle with the rotor speed, and thus the centrifugal force, at the minimum 1 g_m thrust and maximum 12 g_m thrust is shown in figure 12.

Assuming a minimum hinge thickness of one-tenth of an inch, and hinge length of 12 inches, the cross-sectional area is 1.2 square inches. Figure 13 shows that the maximum moment the hinge will be subjected to is 65.3 inch-pounds; under the maximum tensile load, the hinge can withstand 78.1 inch-pounds of bending moment. The average loading will create only 5.1 inch-pounds, while the allowable moment will increase to 96.5 inch-pounds. Since the maximum loading occurs only briefly prior to touch-down, the small margin of safety at that point should be adequate.

Hinge Test Design

Most commercial applications of the integral hinge impose little or no load during flexing, while demanding a large number of flexes. Their most common use at present is in the design of one-piece molded containers with hinged lids.[12]

TABLE 3: CENTRIFUGAL FORCE LOAD ON BLADES

CENTRIFUGAL FORCE = C.F. = $\omega^2 m \int_0^L x\,dx$

WHERE ω = ROTOR ANGULAR SPEED IN RADIANS/SECOND.
m = MASS OF BLADE PER FOOT LENGTH
X = DISTANCE FROM HUB TO ANY POINT ON BLADE
L = LENGTH OF BLADE

ASSUME L = 20 FEET

	ROTOR SPEED (RPM)	BLADE 1 CENTRIFUGAL FORCE (LBF.)	BLADE 2 CENTRIFUGAL FORCE (LBF.)	BLADE 3 CENTRIFUGAL FORCE (LBF.)
AVERAGE	100	125	132	210
MAXIMUM	250	784	826	1315

BLADE 1: INITIAL WEIGHT ALLOTMENT FOR BLADES
3.67 LBF./BLADE

BLADE 2: LIGHTEST OF PROPOSED BLADES
(2 MIL KAPTON, HELIUM INFLATED)
3.86 LBF./BLADE

BLADE 3: HEAVIEST OF PROPOSED BLADES
(3 MIL KAPTON, CO_2 INFLATED)
6.14 LBF./BLADE

FIGURE 12 : VARIATION OF CONING ANGLE WITH ROTOR SPEED

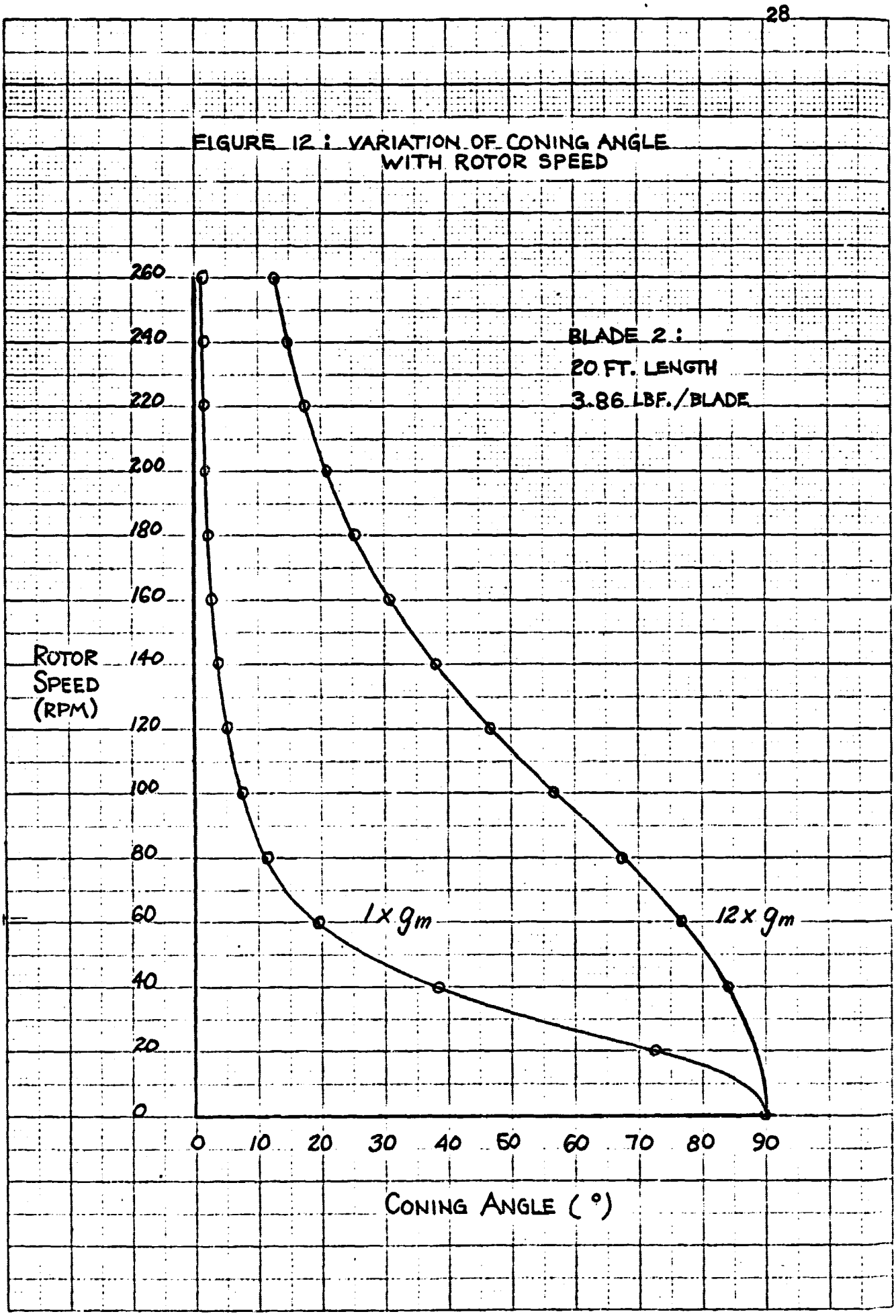

FIGURE 13 : POLYPROPYLENE INTEGRAL HINGE DESIGN

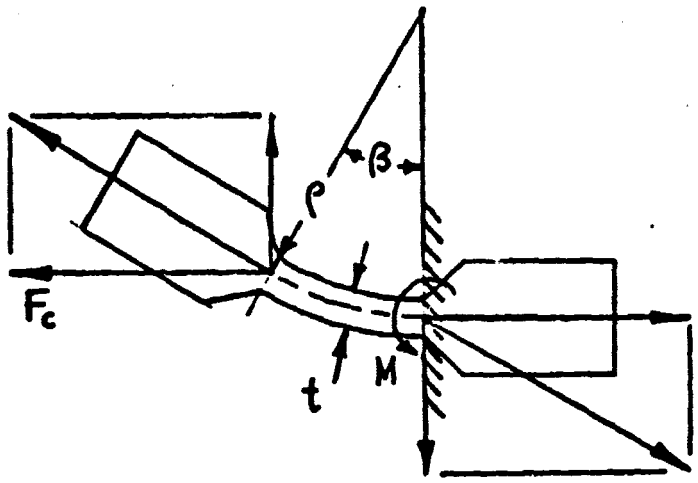

$$M = (F_c \tan\beta)(\rho \sin\beta) - (F_c)(\rho - \rho\cos\beta)$$

AT 250 RPM, $12 \times g_m$ LOAD :

$F_c = 1315$ LB.

$\beta = 14°$

$$\rho = \frac{360°}{14°}\frac{4t}{2\pi} = 1.64 \quad \text{for } t = 0.1 \text{ IN.}$$

$\therefore$ $M_{MAX} = 65.3$ IN.LB.

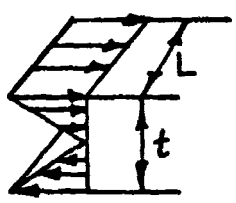

ASSUMING ELASTIC DEFORMATION :

$$M_{ALLOW} = (\sigma_t - \frac{F_c}{A})(L)(\frac{t}{2})(\frac{1}{2})(\frac{2t}{3})$$

FOR $t = 0.1$ IN., $L = 12$ IN., $A = 1.2$ SQ.IN.
$F_c = 1315$ LB., $\sigma_t = 5000$ PSI. (YIELD TENSILE STRESS)

$M_{ALLOW} = 78.1$ IN.LB.

AT 100 RPM, $1 \times g_m$ LOAD :

$F_c = 210$ LB.

$\beta = 8°$

$\rho = 2.55$

$M_{AVE.} = 5.10$ IN. LB.

$M_{ALLOW} = 96.5$ IN. LB.

For application to the autogyro, the hinges must transmit the thrust load developed by the blades to the rotor hub, as well as withstand the much larger centrifugal forces of the spinning blades.

Two polypropylene integral hinge samples were obtained from a plastics manufacturer.* However, no supporting strength or endurance test data was available. In order to ascertain the effect of a steady load on the lifespans of the hinges, a loaded fatigue test was designed and conducted. Since only two hinge samples were available, it was not possible to determine a statistical curve of the results. Therefore, to prove their feasability the samples were tested to the most extreme conditions of the flapping hinge, since this hinge will operate through a greater angular range than the lead-lag hinge. Thus, while the actual hinges will be flexed at an average frequency of 100 cpm, and then momentarily at 250 cpm, the test samples were oscillated at a constant frequency of 250 cpm. The actual cyclic flapping angle is expected to be less than 30°; the test angle was set at 45°.

A weight was suspended from one side of the integral hinge, to simulate the resultant of the blade thrust and centrifugal force; the other half of the hinge was clamped to two pivot edges which were in line with the hinge flexure axis. A crank-rocker, four-bar linkage was designed to flex the hinge from 0° to 45° to 0° for each crank cycle, corresponding to the cyclic blade flapping. The crank was attached to a variable speed electric motor set at 250 rpm. Figure 14 shows a sketch of the proposed test apparatus. Figure 15

*Stokes Molded Products, Trenton, N. J.

FIGURE 14:
PROPOSED BLADE HINGE LOADED FATIGUE TEST

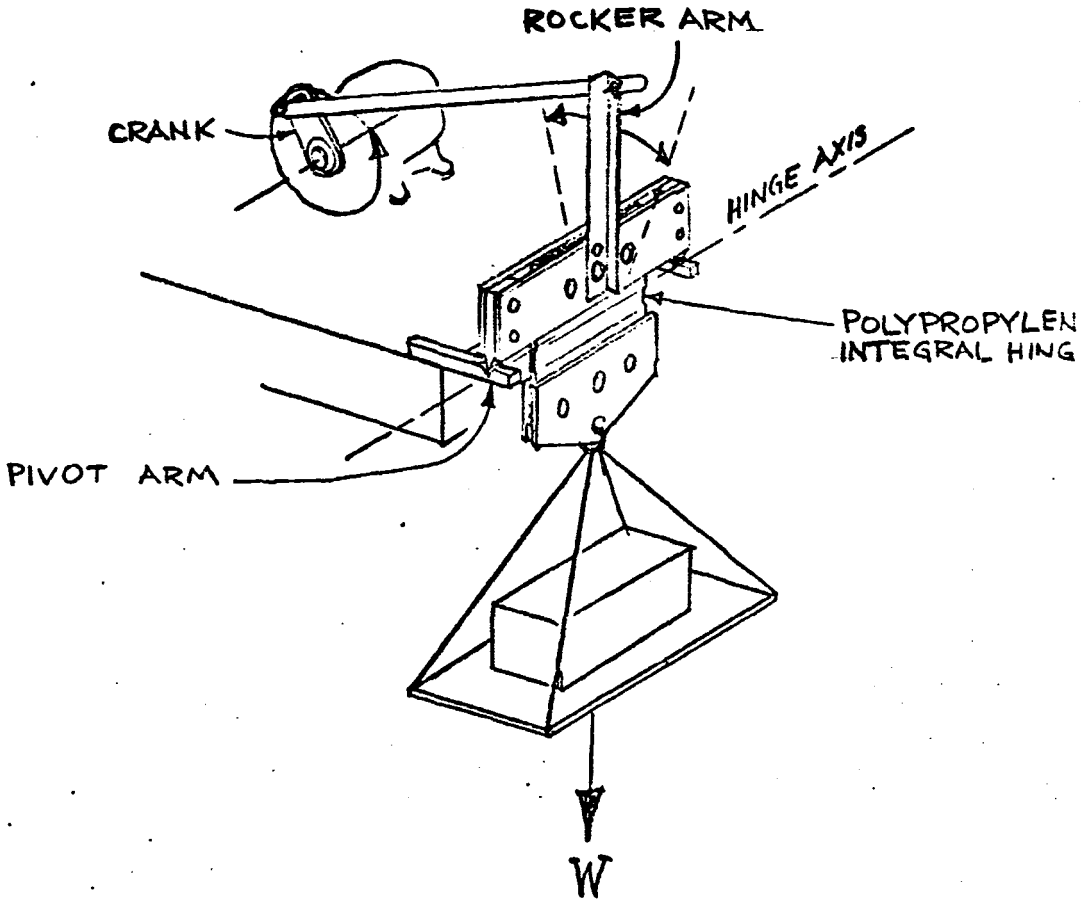

Figure 15: PHOTOGRAPHS OF BLADE HINGE LOADED FATIGUE TEST APPARATUS

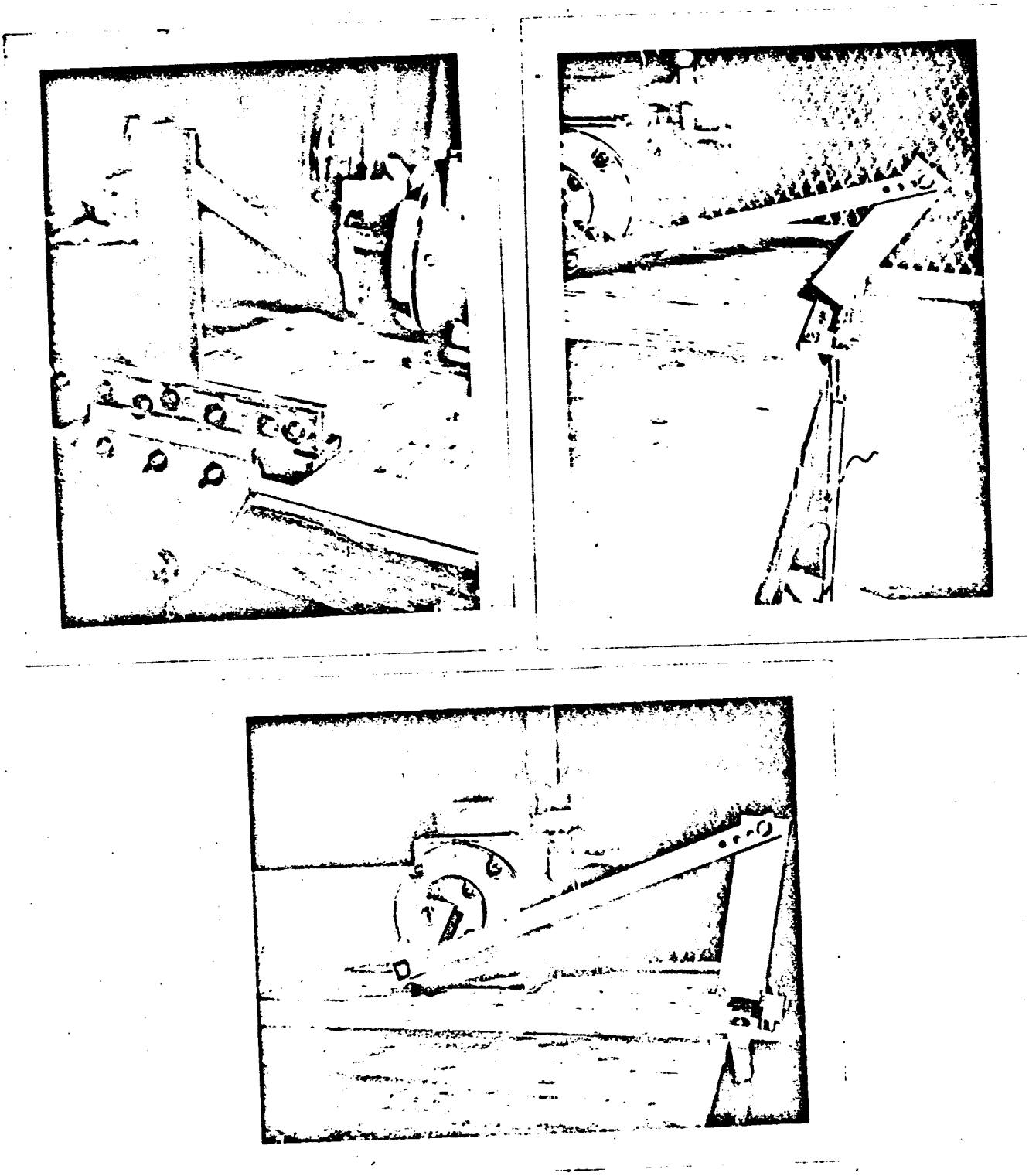

shows photographs of the constructed test apparatus.

Hinge Test Results

The first sample was flexed for 558,750 cycles under a ten pound tensile load. This load corresponds to a tensile stress of 163 psi, nearly the same value as the actual hinge will be subjected to at the 100rpm speed. At this point no signs of failure appeared. The load was then increased to 30 pounds for 200,500 cycles, and then to 70 pounds for 213,750 cycles, at the end of which the hinge failed. Thus, the first hinge sample withstood 973,000 cycles of 45° oscillations, with an increasing load. Table 4 shows the test data derived from the first hinge sample.

The second hinge was loaded with 60 pounds, creating a tensile stress of five times the average stress to be carried by the actual hinges, and 13 pounds less than the load needed to create the maximum stress that the actual hinges must withstand briefly before touch-down. This hinge operated for 988,750 cycles, slightly more than the first hinge, although under a greater load for the first 700,000 cycles. Table 5 lists the test data for the second hinge test.

Since the autogyro blades will rotate less than 2000 cycles during landing, the integral hinge test results indicate the feasability of their use.

TABLE 4:
POLYPROPYLENE INTEGRAL HINGE, LOADED FATIGUE TEST NUMBER 1.

SAMPLE NUMBER	DATE	TIME (MINUTES)	SPEED (RPM)	NO. OF FLEXES	LOAD (POUNDS)	NO. OF FLEXES FOR EACH LOAD
1.	4/25/69	115	250	28,750	10	
	4/28/69	470	250	117,500	10	
	4/29/69	360	250	90,000	10	
	4/30/69	780	250	195,000	10	
	5/1/69	270	250	67,500	10	
	5/2/69	240	250	60,000	10	558,750
	5/5/69	180	250	45,000	30	
	5/6/69	315	250	77,750	30	
	5/7/69	315	250	77,750	30	200,500
	5/8/69	780	250	195,000	70	
	5/9/69	75 FAILURE	250	18,750	70	213,750
					TOTAL →	973,000

TABLE 5:
POLYPROPYLENE INTEGRAL HINGE, LOADED FATIGUE TEST NUMBER 2.

SAMPLE NUMBER	DATE	TIME (MINUTES)	SPEED (RPM)	NO. OF FLEXES	LOAD (POUNDS)	NO. OF FLEXES FOR EACH LOAD
2.	5/14/69	480	250	120,000	60	
	5/16/69	420	250	105,000	60	
	5/19/69	395	250	98,750	60	
	5/20/69	265	250	66,250	60	
	5/21/69	495	250	123,750	60	
	5/22/69	455	250	113,750	60	
	5/23/69	795	250	198,750	60	
	5/26/69	420	250	105,000	60	
	5/27/69	230 FAILURE	250	57,500	60	988,750
					TOTAL →	988,750

VI. COLLECTIVE BLADE PITCH CONTROL

Actuators

The collective blade pitch control actuators were originally to be mounted outboard of the lead-lag hinge for each blade. However, by introducing the use of flexible shafts, the actuators were moved inboard of both the lead-lag and flapping hinges; the thrust bearings in which the blade shafts are mounted remained outboard of the hinges. All three blade pitch angles could now be controlled, via a cable and pulley arrangement, by one actuator mounted on the outside of the outer rotor bearing cone.[17]

Control System

To control the motion of the piston type actuator, a fluidic control system has been proposed.* Two pressure inputs are necessary to operate the system: a constant pressure gas supply, and an alternating reference pressure. The gas supply can be mounted with the fluidic control elements on the outer cone structure; the reference signal must be fed through the rotor bearing from the computer logic inside the capsule. This fluidic link is incorporated in the design of the coning angle indicator linkage discussed in the next section.

*Kershaw, T. N. "Proposed System Analysis of an Autogyro Pitch Angle Control Unit." Interim Report, NASA Grant NGR 33-018-091, July, 1968.

VII. CONING ANGLE MONITOR

Configuration

A major requirement of the rotor hub is the monitoring of the blades' coning angle. Since the revolute bearing would require impractical slip-rings to relay electrical impulses to the capsule computer, a mechanical indicator has been investigated, as follows. Three plastic spars are hinged to the structures just outboard of the blades' flapping hinges, and converge, as an umbrella frame, to the central, vertical indicator rod. The rod, collinear with the rotor bearing axis, moves vertically up and down as the blades cone backward and forward. Extending into the capsule through the rotor bearing's cylindrical neck, the lower end of the rod is attached to a fluidic cylinder position-monitor. See figure 9.

Design Details

The indicator rod is tubular and serves to transmit the reference pressure signal to the collective blade pitch control system mounted on the revolving outer cone structure. To transfer from the non-rotating capsule to the rotating outer cone structure, a swivel seal is incorporated in the indicator rod shaft.

To allow for the cyclic flapping of the blades about any coning angle, the spars are attached to the rod head through ball-and-slot design. Since the coning angle is an average of the positions of the three blades, small

springs anchor the spar balls in the slots and transmit only the average position of the three spars to the indicator rod. See figures 16 and 17.

Constructed from polypropylene, each spar is designed to include an integral hinge, similar to the blade hinges, at the end attached to the blade mounting structure. The indicator rod head is fabricated from nylon or teflon to allow smooth, self-lubricating contact with the spars.

Calibration

To determine the range of motion of the indicator linkage, a half-scale graphical calibration layout was prepared. As shown in figure 18, a coning range of 90° will require a 4.3 inch travel of the indicator rod. The non-linear vertical scale is the averaged position of the indicator rod's centerline for coning angles of 0° to 90°. (Both scales read 10° higher than the actual coning angle since the spars are mounted above the blades' horizontal centerline where the calibration was started.) A flapping angle difference of 50° between any two blades would require 2.6 inches separation on the most expanded segment of the vertical scale. Since the three blades' positions are always averaged, a slide range of two-thirds of this separation must be provided in both directions. Thus, the slides provided in the indicator rod head must allow 3.46 inches total travel for each spar ball.

FIGURE 16: CONING ANGLE INDICATOR AVERAGING CONNECTION

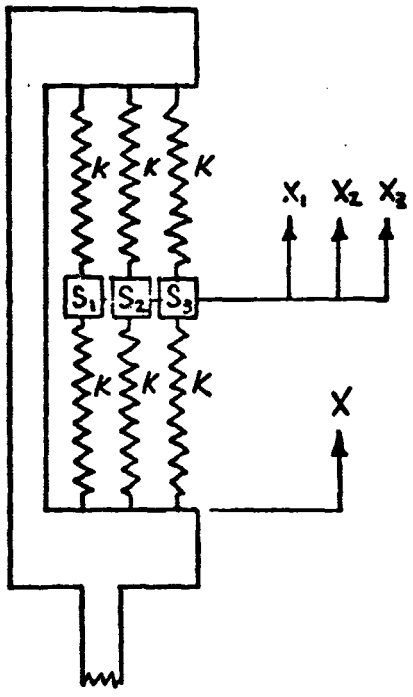

S_1, S_2, S_3 REPRESENT THE MOUNTING POINTS OF THE THREE SPARS.

X_1, X_2, X_3 MEASURE THE MOVEMENT OF THE SPARS IN THEIR SLOTS.

X MEASURES THE RESULTING INDICATOR ROD MOVEMENT.

ASSUMING ALL K'S ARE EQUAL AND CONSTANT,

$$F_1 = 2K(X_1 - X)$$
$$F_2 = 2K(X_2 - X)$$
$$F_3 = 2K(X_3 - X)$$

$\sum F = 0$: $F_1 + F_2 + F_3 = 0$

$$2K[(X_1 - X) + (X_2 - X) + (X_3 - X)] = 0$$
$$X_1 + X_2 + X_3 - 3X = 0$$

REARRANGING YIELDS:

$$X = \frac{X_1 + X_2 + X_3}{3}$$

THUS, THE POSITION OF THE INDICATOR ROD TRANSMITS THE AVERAGE POSITION OF THE THREE BLADE SPARS.

FIGURE 17 : CONING ANGLE INDICATOR, SPAR ROD CONNECTION

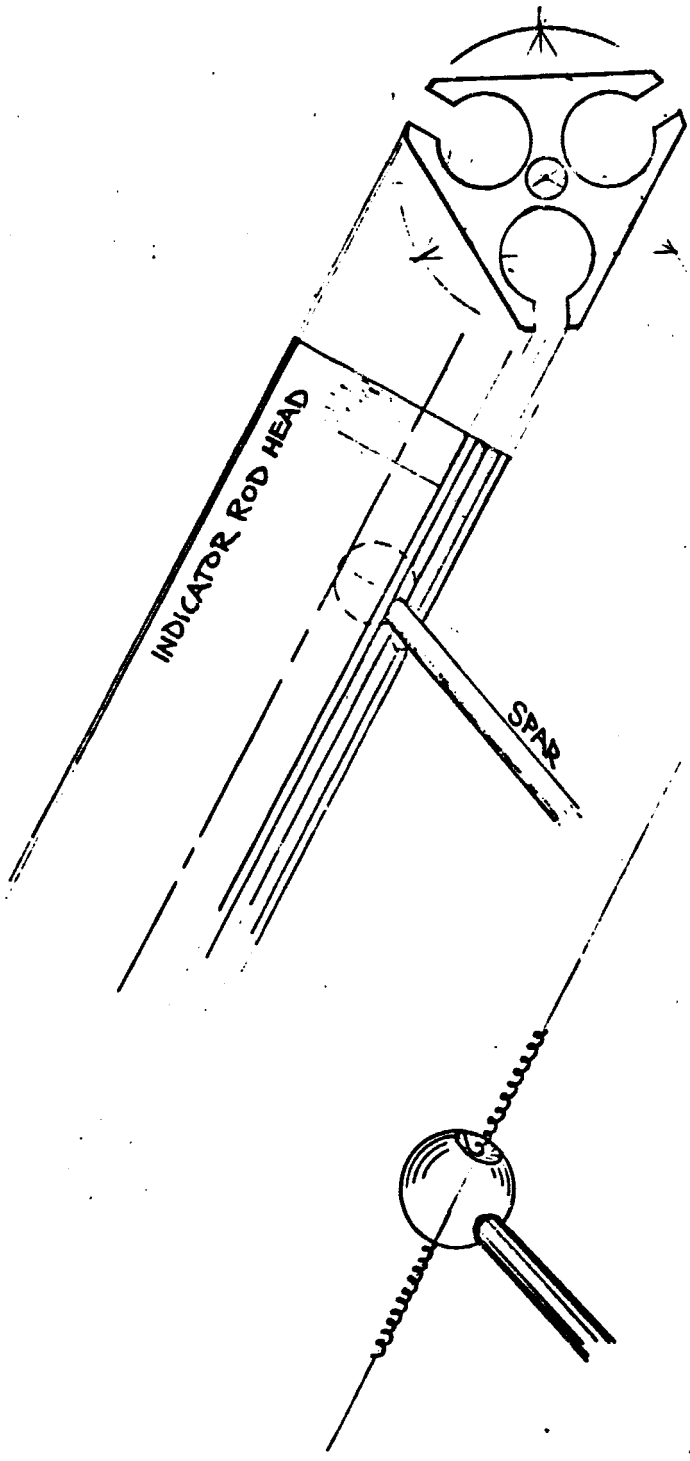

FIGURE 18:
CONING ANGLE INDICATOR
CALIBRATION LAYOUT – 1/2 SCALE

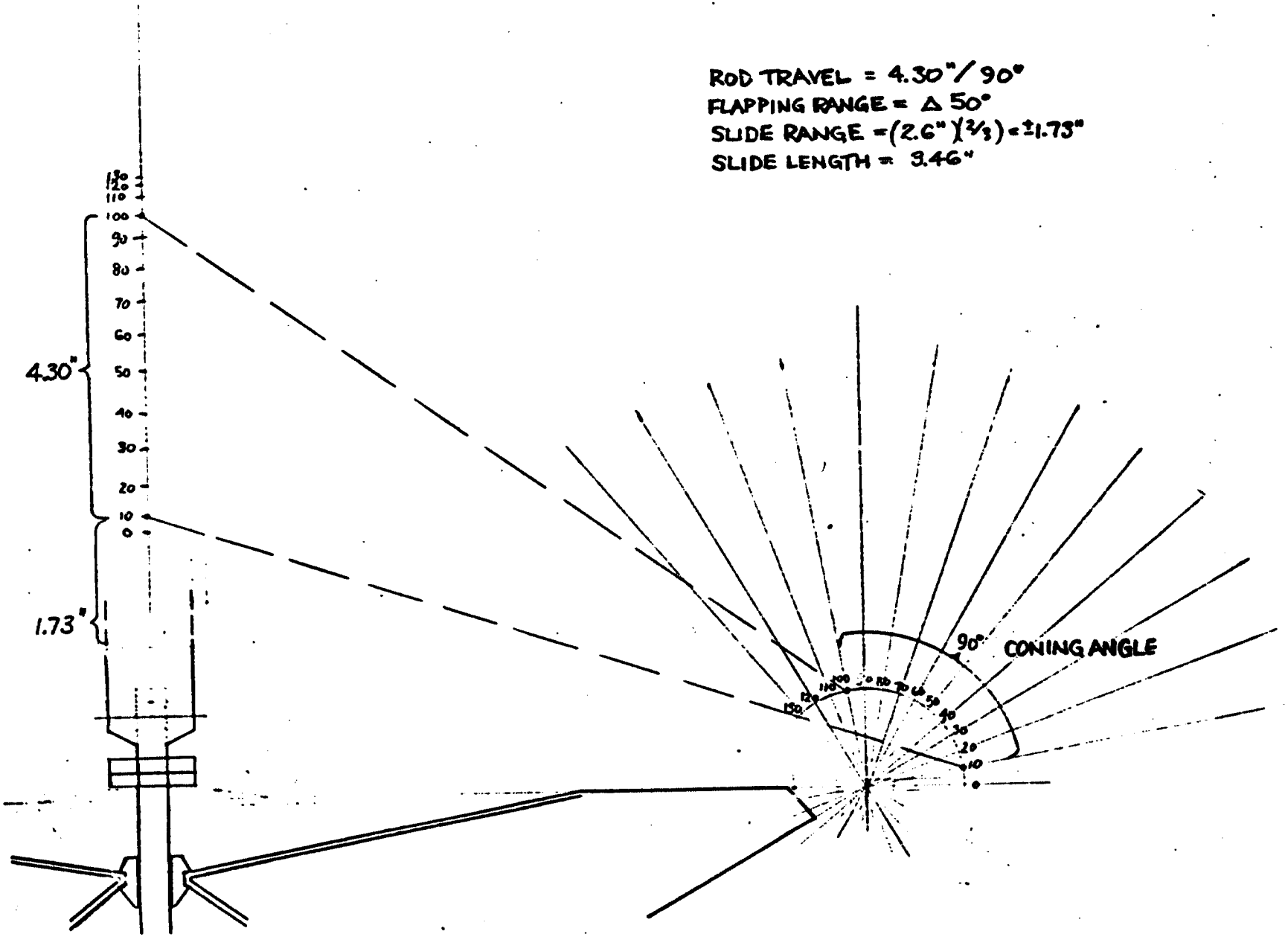

VIII. WEIGHT ANALYSIS

The most stringent factor of the rotor hub design is the lightweight requirement. To help measure the success or usefullness of this design, a weight chart was updated as the design progressed, and greatly influenced the course of the design.

To determine a weight estimate for the rotor-hub assembly, each component was analyzed separately. A stress analysis was used to letermine major dimensions, without analyzing minor design details. Suitable materials were assumed and estimates were made on the conservative side.

The heaviest element of the assembly is the main rotor bearing. To reduce this weight, a large conical angle of 60° was chosen. Furthermore, to maintain the surface tolerances while reducing weight, a cellular structure on the back surface of each cone is recommended. While leaving sturdy radial and circumferential ribs to insure rigidity, much excess material can be milled away between ribs.

Assuming aluminum cones with an average shell thickness of .25 inch, the weight of both cones is 6.56 pounds. Reinforcing the outer rims to support the back-up and reversal bearings on the inner cone, and to carry the blades' horizontal centrifugal loading on the outer cone, requires an additional 1.8 pounds. Additional structural support inside the inner cone is estimated at .5 pound. The back-up and reversal bearings, and the plastic raceway

weigh approximately three pounds. The collective pitch control system is estimated at two pounds, while the cyclic pitch, hub-tilt mechanism and actuator motor will add 2.4 pounds.

The six polypropylene hinges weigh only .8 pound and their intermediary support structure only .5 pound. The coning angle indicator linkage is all plastic except for the tubular indicator rod and averaging springs. The combined weight of this device, including the fluidic monitoring cylinder, is calculated to be less than one-half of a pound.

These weights are outlined in table 6, summing to 19.1 pounds. This figure is based on conservative calculations and estimates. With further design work and test results it is believed that this estimate can be lowered to approximately 15 pounds.

Table 6: Weight Analysis Outline

Rotor Hub Assembly Components	Component Weights in Pounds (earth-weight)		
Main Rotor Bearing			9.6
Inner Cone Structure		4.7	
Cone	3.3		
Inner Support Structure	0.5		
Reinforcing Rim	0.9		
Outer Cone Structure		4.2	
Cone	3.3		
Reinforcing Rim	0.9		
Gas Storage and Supply System		0.7	
Reversal and Back-Up Bearings			2.9
Reversal Bearings (3)		0.4	
Back-Up Bearings (3)		0.4	
Back-Up Bearing Actuating System		0.6	
Raceway Ring		1.5	
Hub Mount and Tilt Structure			2.5
Cylindrical Neck		0.4	
Tilt Bearings and Shaft		0.8	
Tilting Motor and Screw Rod		1.3	
Collective Pitch Control System			2.4
Mechanical Elements		2.0	
Fluidic Control Elements		0.4	
Blade Hinge Structure			1.3
Hinges (6)		0.8	
Hinge Support Structures (3)		0.5	
Coning Angle Indicator Linkage			0.4
Indicator Rod		0.0	
Spars		0.1	
Rod Head		0.1	
Swival Seal		0.1	
Fluidic Monitoring System		0.1	

Total Calculated And Estimated Weight Of Present Design = 19.1 pounds

IX. LITERATURE CITED

1. Azuma, A. "Dynamic Analysis of Rigid Rotor Systems." Journal of Aircraft, Volume 4 (May, June, 1967). 203-9.

2. Barzda, Justin J. "Rotors for Recovery." Journal of Spacecraft, Volume 3 (January, 1966). 104-9.

3. Baum, Bernard. "Designing with Cast Nylon." Modern Plastics, April, 1968. 173-178.

4. Braund, H. M., R. E. Darnall, T. N. Kershaw, and G. N. Sandor. "Analysis and Design of a Capsule Landing System and Surface Vehicle Control System for Mars Exploration." NASA Grant NGR 33-018-091, June 16, 1968.

5. Brunelle, E. J., T. N. Kershaw, W. P. Rayfield, and G. N. Sandor. "Landing on Mars by Autogyro." Rensselaer Review of Graduate Studies, No. 53 (October, 1968). 19-23.

6. Cadmen, R. V. "Rolamite - Geometry and Force Analysis." ASME, Paper No. 68 - Mech - 17. Presented October, 1968.

7. Casani, E. K. "Entry and Landing Capsule System." J.P.L. Space Programs Summary, 37-52, Volume III. 21-5.

8. Freundlich, M. M., and C. H. Hannan. "Problems of Lubrication in Space." Lubrication Engineering, February, 1961.

9. Grassam, N. S., and J. W. Powell, editors. Gas Lubricated Bearings. London: Butterworths, 1964. 110-39.

10. Gross, W. A. Gas Film Lubrication. New York and London: John Wiley and Sons, Inc., 1962. 255-306.

11. Morris, A. C., and A. Richardson. "Polypropylene: Creep and Impact Data." British Plastics, Volume 41 (March, 1968). 92-7.

12. Morris, A. C., and A. Richardson. "Polypropylene in Injection Moulded Applications." British Plastics, Volume 41 (July 1968). 87-90.

13. Pan, Coda H. T., and Peter H. Broussard, Jr. "Squeeze-film Gas Lubrication." NASA Technical Memorandum, X - 53618 (June 8, 1967).

14. Sadler, J. Peter. "The Study of Design and Fabrication Properties of an Inflatable Rotor Blade." Master of Engineering Project, Rensselaer Polytechnic Institute, 1969.

15. Simonds, Herbert R., and James M. Church. A Concise Guide to Plastics. New York: Reinhold Publishing Corporation, 1966. 200.

16. Ward, J. F. "Summary of Hingeless-rotor Structural Loads and Dynamics Research." Journal of Sound and Vibration, Volume 4 (November, 1966). 358-77.

17. Wepner, R. "Blade Support and Pitch Control." Master of Engineering Project, Rensselaer Polytechnic Institute, 1969.

18. Williams, H. "Lubricants Limit Ball Bearings for Space Craft." Space/Aeronautics, February, 1962.